



3D Composite scaffolds using strontium containing bioactive glasses

Melek Erol*, Ayşe Özyuğuran, Özlem Özarpat, Sadriye Küçükbayrak

Istanbul Technical University, Chemical Engineering Department, 34469 Maslak, Istanbul, Turkey

Abstract

In this study, it was aimed to fabricate and characterize three-dimensional composite scaffolds derived from Sr-doped bioactive glass for bone tissue engineering applications. The scaffolds were fabricated by using polymer foam replication technique and coated with gelatin to be able to improve the properties of them. The porous scaffolds were successfully synthesized using optimized process parameters. Both coated and uncoated scaffolds favored precipitation of calcium phosphate layer when they were soaked in simulated body fluid (SBF). Gelatin coating improved the mechanical properties of the scaffold and also it did not change the bioactive behavior of the scaffold. It was observed that there was a good pore interconnectivity maintained in the scaffold microstructure. Results indicated that scaffolds can deliver controlled doses of strontium toward the SBF medium. That is the determinant for bone tissue regeneration, as far as strontium is known to positively act on bone remodeling.
© 2012 Elsevier Ltd. All rights reserved.

Keywords: Scaffold; Sintering; Glass; Biomedical applications

1. Introduction

Scientists have been carrying out various studies to maintain quality of life of the human being. One of them is repairing bone defects like cracks and fractures, which occur via natural processes or other reasons. One of the solutions is bone transplantation. But there are some limitations such as lack of donors and morbidity of the donor site.¹ Implantation with bioinert materials leads to loss of bone density. In addition, these materials eventually need to be replaced. Bone tissue engineering is a rapidly developing discipline with the intension to repair, replace or regenerate injured bone tissues with the aid of biodegradable scaffolds. The advantage of this approach is the reduced number of operations needed, resulting in a shorter recovery time for the patient.^{2,3}

A key component in tissue engineering for bone regeneration is scaffolds, which mimic the structure of bone mineral and act as templates for desired cell responses. Among a variety of materials for the scaffold preparation, bioactive glasses exhibit great performances for bone tissue regeneration because they are bio-compatible, bioactive, osteoconductive and osteopductive.^{4,5} These materials are able to bind with bone through a layer of hydroxyapatite formed on their surfaces when they are implanted

in human body.^{6–8} Bioactive glasses, discovered by Hench in 1969,⁹ and related silicate glass–ceramics, constitute thus a group of inorganic materials being highly considered in tissue engineering due to their high bioactivity.^{10–12} Bioactive glass of composition 45S5 Bioglass® (in wt%: 45% SiO₂, 24.5% Na₂O, 24.4% CaO and 6% P₂O₅) exposes critical concentrations of Ca²⁺, Si⁴⁺, Na⁺ and P⁵⁺ ions which have been shown to activate genes in osteoblast cells thus stimulating new bone formation *in vivo*.^{13,14} Bioactive glasses are also reported to stimulate angiogenesis.^{15,16} In order to improve bone production properties of these biomaterials, bone cell stimulator ions can be incorporated into their chemical compositions. Strontium is known to accelerate bone healing processes and have positive effects on bone tissue repair.¹⁷ *In vitro* and *in vivo* studies have indicated that strontium increases bone formation and reduces osteoporosis, leading to a gain in bone mass and improved bone mechanical properties in normal animals and humans.^{18–22} Moreover, Gentleman et al.²³ have shown that ion release from Sr-doped silicate glasses enhances bone cell activity. *In vivo* studies have also confirmed the high biocompatibility of Sr-containing 45S5 Bioglass® expressed through strong bonding to bone via HCA layer without any inflammatory affects.²⁴ Several studies show that the Sr-containing hydroxyapatite (Sr-HA) and bioactive glasses promote osteoblast attachment and mineralization *in vitro* and bone growth and osteointegration *in vivo*.^{25–34} In contrast to these superior properties, inorganic scaffolds made of bioactive glasses suffer from low mechanical strength and high

* Corresponding author. Tel.: +90 212 2857345; fax: +90 212 2852925.
E-mail address: erolm@itu.edu.tr (M. Erol).

brittleness. It is known that the high tensile strength and fracture toughness of bone are strongly correlated to the presence of the collagen fibers.³⁵ Based on this knowledge, brittle scaffolds can be coated with polymer layers in order to improve their mechanical properties. It is proposed that polymer filaments will bridge cracks during fracture thus increasing the scaffold toughness, in a similar manner as collagen fibers enhance the fracture toughness of bone.³⁵ The approach has been extended to include scaffolds with interpenetrating network structures, where the polymer is added not only as a surface coating but is also made to penetrate and infiltrate the pore walls (struts) of the scaffold via remaining porosity or microcracks.³⁶ The concept of polymer coating and formation of interpenetrating polymer–ceramic microstructures has also been applied to scaffolds made from HA, alumina and bioactive glasses. Peroglio et al.³⁷ have recently investigated alumina scaffolds coated with PCL. It was reported that the PCL coated alumina scaffolds led to a 7- to 13-fold increase of the apparent fracture energy. The authors also showed that toughening is due to crack bridging by polymer fibrils. Chen et al.³⁸ reported that coating Bioglass® scaffolds with PDLLA leads to a sevenfold improvement of the work of fracture. In a similar study, Mantsos et al.³⁹ investigated the effect of PDLLA coating on scaffolds fabricated from boron containing bioactive glasses and showed that the compressive strength of PDLLA-coated scaffolds being 30–50% higher than that of the uncoated scaffolds. Work by Nalla et al.^{40,41} has investigated the toughening mechanisms in bone and dentin by collagen interaction with microcracks in the inorganic phase. The role of collagen fibrils providing a crack bridging mechanism was postulated.⁴¹ It is also reported that collagen derived gelatin is biodegradable, biocompatible, non-cytotoxic, with an ability to support cellular growth. Because of these superior properties gelatin has a wide application range within the field of both soft and hard-tissue engineering.⁴² Production of scaffolds from bioactive glasses or their composites with polymers is thought to be promising in terms of mechanical, bioactive and osteoproduative properties. To the author's knowledge there has been not any study on the fabrication of scaffolds with Sr-containing bioactive glasses coated with gelatin for bone tissue engineering applications. In this study, strontium-containing bioactive glasses were used to fabricate three-dimensional (3D) scaffolds for bone tissue engineering applications. The scaffolds were then coated with collagen derived gelatin and their structural, physical and mechanical properties were investigated.

2. Materials and methods

2.1. Materials

Gelatin was purchased from Sigma–Aldrich Ltd. (Dorset, UK). The bioactive glass powder used for fabricating the scaffolds was produced in a previous study.⁴³ The nominal composition of this glass in weight % is 45% SiO₂, 24.5% Na₂O, 6% P₂O₅, 2% SrO and 22.5% CaO. Sr-doped glasses were used in the fabrication of 3D scaffolds. All other chemicals used were of analytical grade.

2.2. Scaffold fabrication

Scaffolds were prepared using a polymer foam replication technique, as described in detail elsewhere.¹⁰ Briefly, a 50 ml volume of slurry was prepared using PVA which was dissolved in deionized water for 1 h at 80 °C. Afterwards glass powder were dispersed into the solution under constant stirring. The composition of the slurry is 5% PVA, 60% water and 35% glass powders. A polyurethane foam (PU, 60 ppi) with a structure comparable to that of human trabecular bone was used as a sacrificial template for the replication method. The foam was cut into samples of dimensions 10 mm × 10 mm × 10 mm. Foams were immersed in the slurry for 3 min so that foam struts were coated with bioactive glass particles. The as-coated foams were then dried at room temperature overnight and then subjected to a controlled heat treatment. The samples were heated at 2 °C/min to 550 °C in air to decompose the foam, then at 2 °C/min to 950 °C, and kept at this temperature for 2 h to densify the glass network. The scaffolds were then coated with gelatin (Type A and Type B). The coated scaffolds were left to dry at 37 °C for 1 h and subsequently at room temperature overnight.

2.3. Characterization

2.3.1. Porosity

Porosities of the coated and uncoated scaffolds were measured by Mercury Intrusion Porosimetry, using a Quantachrome Poromaster series. Data on percent porosity were acquired through a microcomputer data acquisition system interfaced with the porosimeter.

2.3.2. Surface morphology

Scanning electron microscopy with energy dispersive spectroscopy (SEM-EDS) capability (JEOL 5410) was used for the morphological and elementary characterization of coated and uncoated scaffolds. Samples were fixed on a SEM sample holder, air dried under vacuum and coated with a thin layer of gold.

2.3.3. Structural analysis

X-ray diffraction (XRD) analysis of the coated and uncoated 3D scaffolds was performed using PANalytical X'Pert Pro diffractometer to investigate the characteristic phases and possible crystallinity of the fabricated samples. Data were obtained over the range $2\theta = 5\text{--}60^\circ$ using a step size of 0.04° and counting time of 25 s per step employing Cu K α radiation (at 40 kV and 40 mA). Fourier-Transform Infrared Spectroscopy (FT-IR) spectra were collected using a Perkin Elmer Spectrum 100 Model spectrometer in transmittance mode in the mid-IR region ($4000\text{--}650\text{ cm}^{-1}$). For XRD and FT-IR measurements, the samples were ground and measured in powder form.

2.3.4. Mechanical properties

The compressive strength of samples (dimensions: 5 mm × 5 mm × 10 mm) was measured using a Shimadzu AGS-J servo-hydraulic testing instrument. The crosshead speed

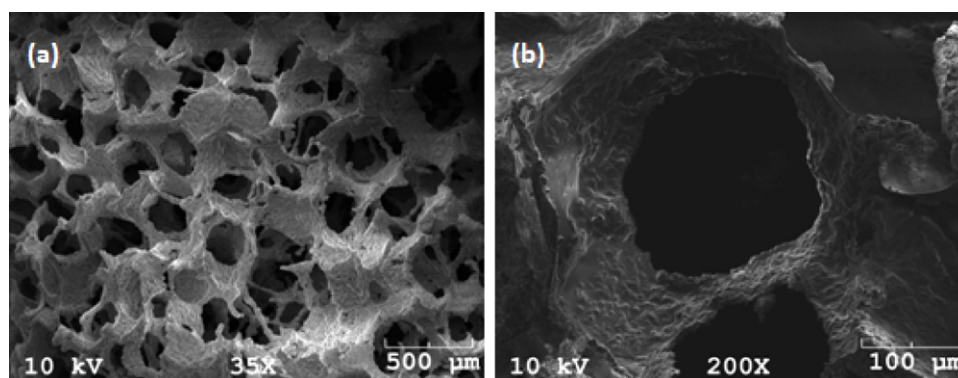


Fig. 1. SEM images showing the pore (a) and strut (b) microstructures of a scaffold produced by the foam replica method and sintered at 950 °C for 2 h.

was 0.5 mm/min with a pre-load of 1 N. At least five specimens for each sample series were tested. Average values and standard deviations were determined.

2.3.5. Assessment of bioactivity

The test of the acellular bioactive behavior of scaffolds was performed *in vitro* through the immersion of samples in SBF, as described by Kokubo et al.⁴⁴ Each sample of dimensions 5 mm × 5 mm × 5 mm was immersed in 30 ml of SBF and was stored in an incubator at controlled temperature of 37 °C. Samples were immersed in SBF for different soaking periods: 1, 7, 14 and 28 days. When samples were removed from the SBF solution, they were rinsed with ethanol and water, and dried at 37 °C for 30 min. The samples were then characterized using SEM and XRD.

2.3.6. Strontium release investigation

Changes in the concentration of strontium in the SBF solution as a result of the soaking of scaffolds for 1, 7, 14 and 28 days were measured using inductively coupled plasma optical emission spectrometry (ICP-OES). A Perkin Elmer Model Optima 2100 ICP operated at 13.56 MHz (using Ar and N₂ gases) was used for the measurements.

3. Results and discussion

3.1. Microstructural characterization

Visual inspection of the obtained scaffolds showed that the scaffolds preserve their initial shape, without collapsing the macroporous structure. The macroporous network and the strut microstructure of uncoated and coated scaffolds can be seen in Figs. 1 and 2, respectively. Highly porous scaffolds with interconnected porosity were produced. Inspection of SEM images indicates that gelatin has attached onto the bioactive glass scaffold surface forming a uniform coating without blockage of the pores, as observed in Fig. 2. It can be clearly seen that the interconnected porosity is also maintained after polymer coating. The strut microstructure can be seen in Figs. 1(b) and 2(b). The microstructure of the sintered struts indicates that significant sintering has occurred and this result confirms that the sintering parameters have been correctly chosen. It is also observed in Fig. 2(b) that the gelatin coating covered fairly uniformly the surface of the struts and the glass grain morphology is not clearly visible, which indicates a homogeneous distribution of the polymer coating on the surface of the scaffold. According to the SEM observations, it can be confirmed that the interconnected character of the porosity and the pore size of the scaffolds coated with gelatin are suitable for cell attachment,

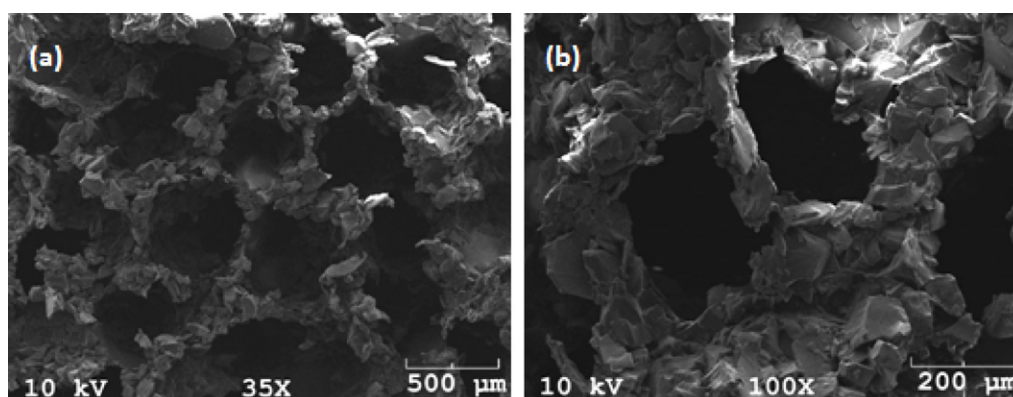


Fig. 2. SEM images showing the microstructure of a scaffold coated with gelatine at (a) low and (b) high magnifications.

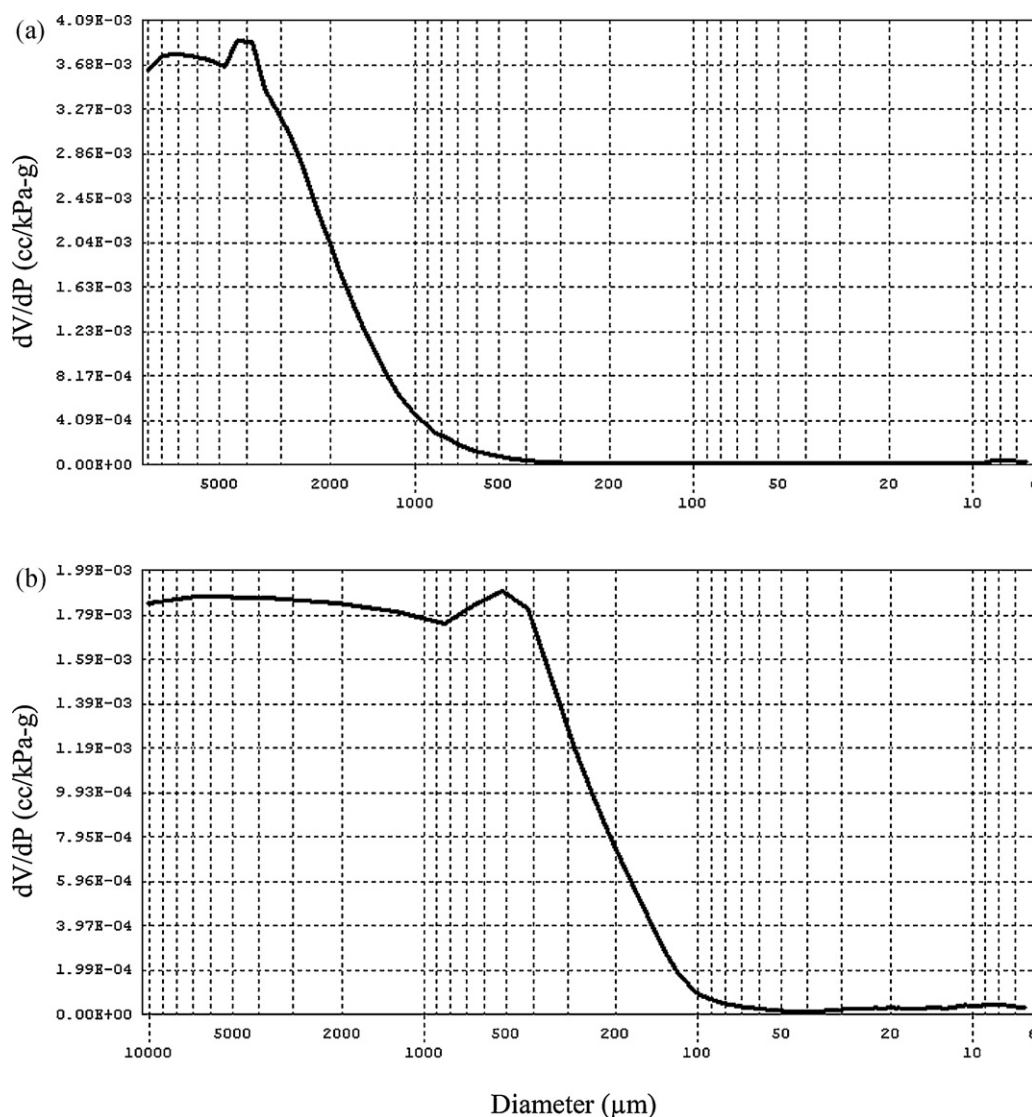


Fig. 3. Pore size distributions of uncoated (a) and coated (b) scaffolds.

migration and vascularization.⁴⁵ The porosities of the coated and uncoated scaffolds were measured as $89\% \pm 2.2\%$ and $79\% \pm 1.9\%$, respectively. As expected the porosity of the scaffold decreased because of the gelatin coating. However, the porosity of the coated scaffolds is still good enough for the bone tissue engineering applications.⁴⁵ The pore size distributions of the coated and uncoated scaffolds are also given in Fig. 3. It is clear that the pore size range of the uncoated scaffolds is extremely wider than that of the coated one. The average pore size of the coated scaffold was found to be $\sim 500 \mu\text{m}$, with a range of 380–875 μm , which is in the size range desired for application as a bone tissue engineering scaffold.⁴⁶ Pore sizes smaller than 100 μm should be avoided for applications in bone tissue engineering.⁴⁷ Therefore, coated scaffold indicates the suitability of the scaffold for cell attachment, migration and vascularization.

3.2. Structural analysis

Fig. 4 shows the transmittance spectra of uncoated and coated scaffolds. The characteristic spectrum exhibits peaks in the range 1022–1110 cm^{-1} assigned to the Si–O bending mode and the characteristic peak of the modified silicate network is seen at $\sim 910 \text{ cm}^{-1}$.^{48–50} The respective spectrum of the sample indicates all the features assigned to the glass network. The major peaks in the range 3600–3000 cm^{-1} are attributed to the unsaturated asymmetric O–H stretching vibration.^{25,48} Furthermore, the big peak at $\sim 1590 \text{ cm}^{-1}$ can be assigned to the N–H bending vibration of amine groups in gelatin.⁴⁸ This result also showed that the scaffold successfully coated with gelatin.

Fig. 5 indicates the XRD patterns of the uncoated and coated scaffolds. As can be seen from Fig. 5 the amorphous state of the bioactive glass still remained after sintering. There is only

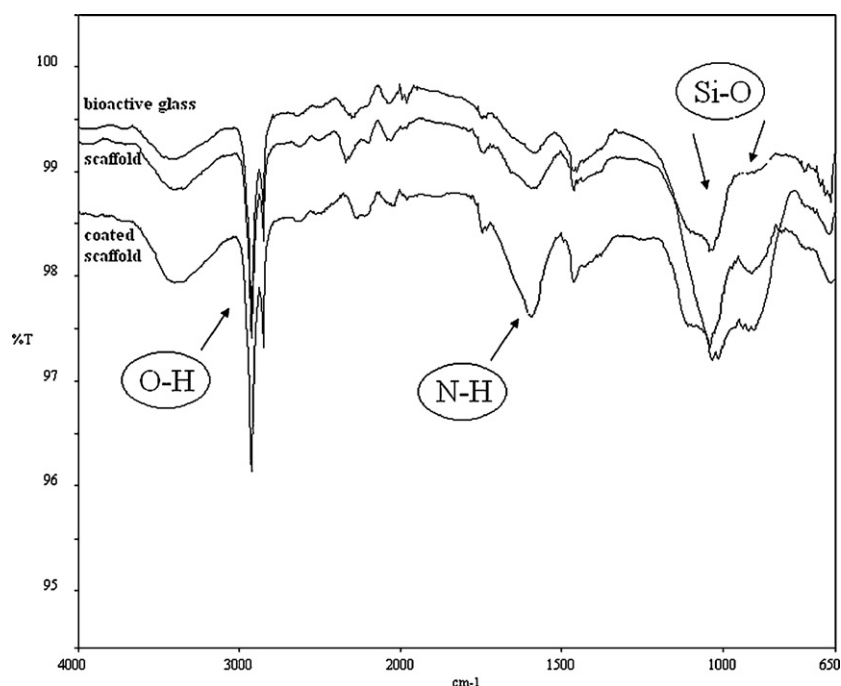


Fig. 4. FT-IR spectra of the scaffolds and bioactive glass.

one small crystalline peak at $2\theta = 33^\circ$ which is attributed to $\text{Na}_2\text{Ca}_6(\text{Si}_2\text{O}_7)(\text{SiO}_4)_2$ crystalline structure. The detailed DTA study was performed in the previous study.⁴³ It was found that there were one shallow endothermic peak at 558°C , which shows the glass transition temperature and one exothermic peak at 839°C corresponding to the crystallization temperature. It is obvious that the sintering temperature of 950°C is not enough for the fully crystallization. Therefore, partial crystallization occurred in the scaffolds. It is known that 45S5 Bioglass[®] may have potential limitations as scaffold material for bone repair and regeneration due to the tendency of the glass to crystallize before appreciable viscous flow during scaffold fabrication.^{51–53} It is not possible to sinter 45S5 Bioglass[®] particles into a porous 3D network with adequate strength for repairing bone defects

and to keep the amorphous glass structure. It is known that an amorphous phase is less stable than its crystalline counterpart, which is expected to result in better bioactive behavior in comparison to partially crystallized scaffolds. Furthermore, the structure of scaffold did not change after coating with gelatin. This result confirms that no or negligible chemical reaction occurred between the sintered bioactive glass and the gelatin.

3.3. Mechanical behavior

Compressive strength values of uncoated and coated scaffolds were calculated as 0.1 ± 0.05 MPa and 1.4 ± 0.09 MPa. It is clear that the compressive strength of the scaffolds increased by coating with gelatin when compared with uncoated scaffolds. It is suggested that the gelatin layer covers the struts and fills the microcracks situated on the strut surfaces improving the mechanical stability of the scaffold. Mechanical strength of the polymer/bioactive glass composite scaffolds has been studied widely and the similar results were reported.^{36,54,55} The measured compressive strength value for the coated scaffold falls close to the lower bound of the values for spongy bone. The compressive stress–strain curves are given in Fig. 6 for uncoated and coated scaffolds. The compression strength was taken in each case as the highest value of stress before the collapse of the scaffold structure. As seen by the change of slopes, scaffolds are already damaged before failure due to the pre-load applied on them. This phenomenon is more prominent for the stress–strain curve of the coated scaffold. However, it is clear that coated scaffolds can withstand higher strains before progressive failure occurs. Coating with gelatin leads to a 14-fold improvement of the work of fracture. The presence of the gelatin has been shown to lead to toughening of the structure, and crack bridging by polymer fibrils has been identified as being the most likely

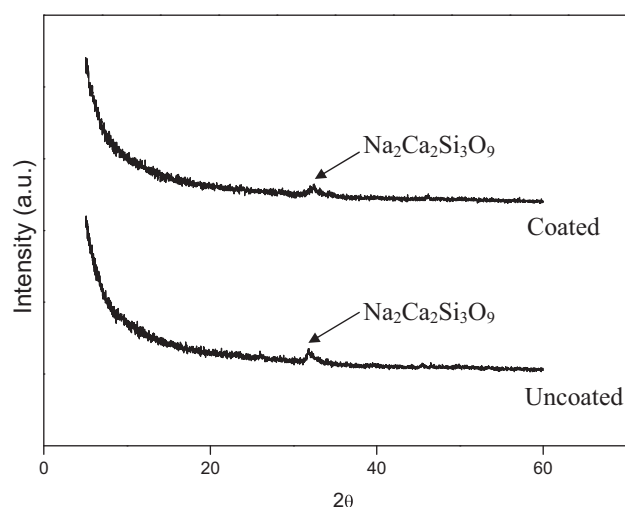


Fig. 5. XRD patterns of uncoated and gelatine coated samples.

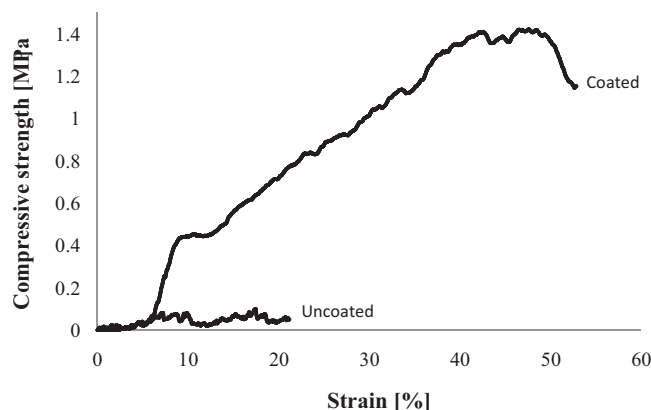


Fig. 6. Stress–strain curves of the coated and uncoated scaffolds.

toughening effect.^{36,56} Therefore, it can be proposed that the compressive strength value of the coated scaffold is sufficient for the scaffolds to be handled safely in the laboratory and for effective manipulation for *in vivo* studies.

3.4. Bioactivity assessment

SEM and XRD analyses were carried out to detect the HA layer formed on the surface of the both coated and uncoated scaffolds in contact with SBF. Figs. 7 and 8 show the gradual development of a HA layer, as confirmed by XRD analyses, on the surface of the uncoated and coated scaffolds following increasing days of immersion in SBF. As seen in figures, small peaks at 32° and 34° 2θ were detected in XRD patterns of bioactive glass samples soaked in SBF starting from the first day. These peaks were assigned to HA [$\text{Ca}_{10}(\text{PO}_4)_6(\text{OH})_2$] and [$\text{Ca}_5(\text{PO}_4)_3(\text{OH})_2$] according to the standard JCPDS cards (09-4-0432) and (01-073-1731), respectively. It is apparent that an HA layer was formed on the surface of the scaffolds after 1 day in SBF. Both coated and uncoated scaffolds are highly bioactive materials.

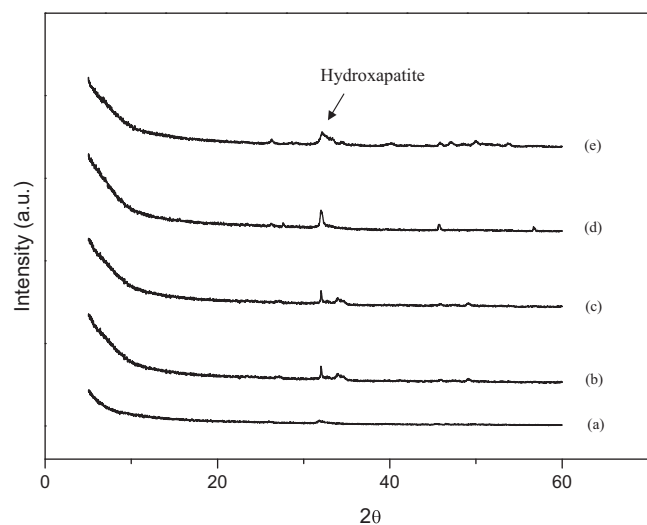


Fig. 7. XRD patterns of uncoated scaffold before (a) and after (b) 1, (c) 7, (d) 14 and (e) 28 days immersion in SBF.

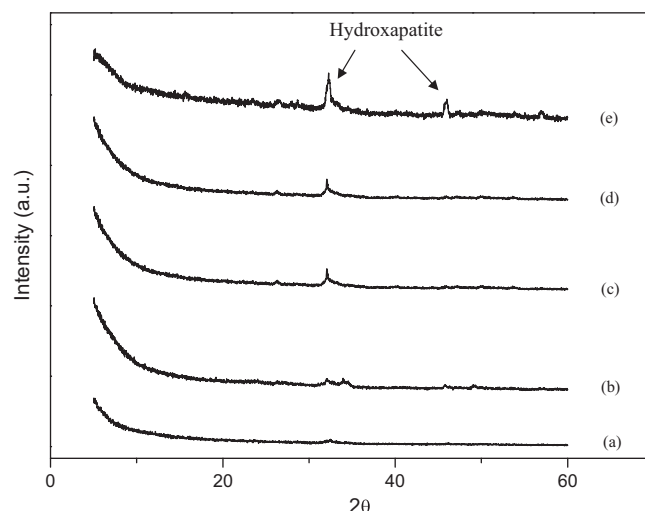


Fig. 8. XRD patterns of gelatine coated scaffold before (a) and after (b) 1, (c) 7, (d) 14 and (e) 28 days immersion in SBF.

SEM micrograph of a coated scaffold after 7 days of immersion in SBF can be seen from Fig. 9. It is clear that HA crystals are formed as a result of the contact of the bioactive glass struts with SBF. The process of HA formation is based on the ionic exchange between the scaffold surface and the SBF solution, which is the well-known mechanism proposed for bioactive glasses by Hench.⁶ In the first stage, an interchange between the Ca^{2+} ions of the produced samples and the H_3O^+ ions of the solution takes place. This is followed by a breakdown of the silica network, forming silanol bonds that repolymerize to form a hydrated, silica rich layer, resulting apatite layer. At the final stage, nucleation and growth of the HA crystals on the top of this silica-rich layer are observed.⁶ It can be clearly seen that the HA layer was homogeneously covered the surface of the scaffold in contact with SBF while the gelatin coating cannot still be observed on the surfaces of the struts. The formation of HA on the surfaces of coated scaffold after immersion in SBF was confirmed also by EDX analysis (shown in Fig. 9c). High Ca and P peaks belonging to HA were detected. After SBF immersion, Ca/P ratio of 2.08 is close to the stoichiometric value (1.67) of hydroxyapatite ($\text{Ca}_{10}(\text{PO}_4)_6(\text{OH})_2$). This result is also confirmed the presence of HA layer on the surface of the coated sample immersed in SBF. However, high Ca/P ratio also shows the high amount of calcium comparing to the amount of phosphorous. High calcium amount was detected on the surface of the scaffolds since the glass contains much more calcium than phosphorous.

3.5. Strontium release

Fig. 10 shows the cumulative concentration of Sr^{2+} ions released from the coated and uncoated scaffolds into the SBF solution. A rapid increase in the strontium concentration occurred for uncoated scaffold because of the higher rate of glass dissolution process compared with the coated one. Glass dissolution is lower for the coated scaffold probably due to formation of gelatin layer onto the surfaces of the scaffold. Sr-doped

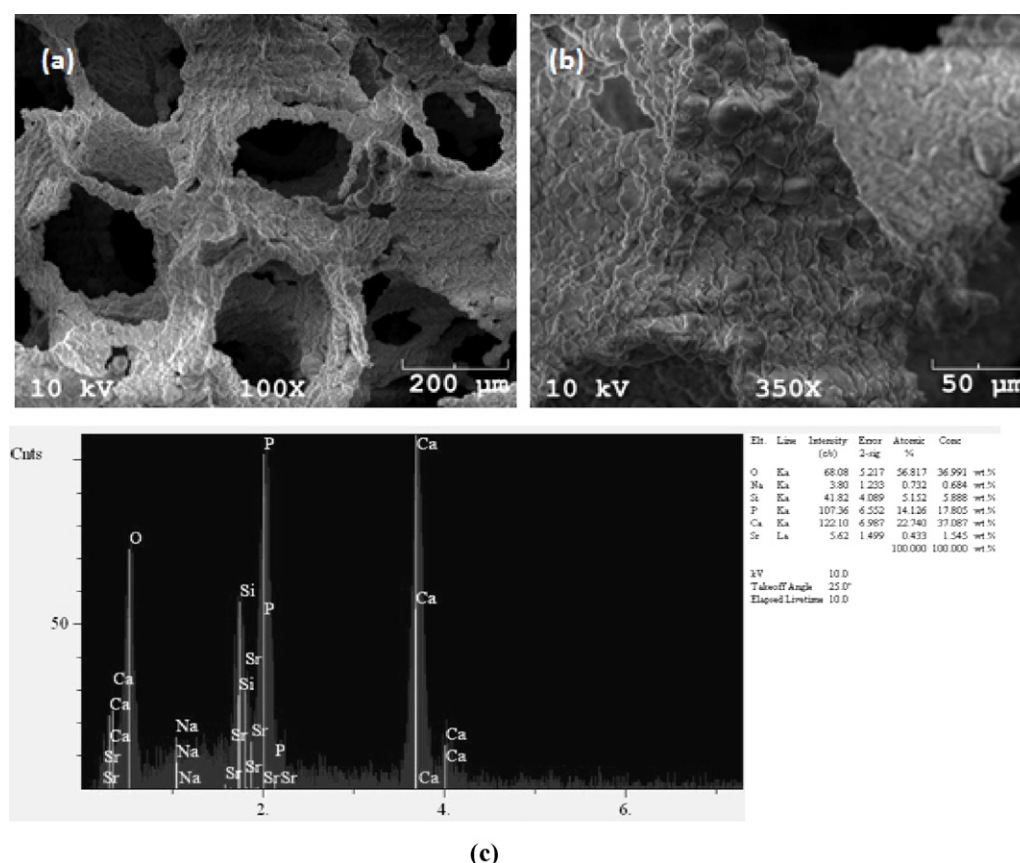


Fig. 9. SEM image showing the surface of gelatine coated scaffold after 7 days of immersion in SBF.

glasses have been shown to exhibit enhanced acellular bioactivity and inhibited osteoclasts differentiation and to release concentrations of Sr^{2+} ions in the range of 5–23 ppm into the dissolution medium.²³ It was also reported that Sr^{2+} ion levels induced stimulatory effects on osteoblasts range from 8.7 to 87.6 ppm.^{57,58} Some evidence has also indicated that very high doses of Sr^{2+} ion may induce mineralization defects.⁵⁹ The higher the strontium level the more pronounced the inhibitory effect on osteoclast differentiation and resorption up to levels as high as 2102.8 ppm.^{57,60} Possible burst release and higher

concentration of strontium could be cytotoxic and provide unfavorable conditions for cell attachment and growth. Therefore, it is proposed that the slow release of strontium, as observed in coated scaffold, is favorable for the possible tissue engineering applications of the present scaffolds. It can be said that coated scaffold may have therapeutic potential with respect to the Sr^{2+} ion release profile detected in this study.

4. Conclusions

Bioactive and mechanically robust porous 3D scaffolds have been successfully synthesized by the replication technique using strontium containing silicate glass. Both uncoated and coated scaffolds exhibit highly bioactive behavior, confirmed by the rapid growth of an HA layer after 1 day of immersion in SBF. It is clear that the gelatin coating did not change the bioactive behavior of the scaffold. Furthermore, gelatin coating significantly improved the compressive strength values of the scaffold. This investigation introduced for the first time the application of Sr-doped bioactive glass for the fabrication of 3D porous structures, which remain in mostly amorphous glass state and exhibit all the necessary characteristics and parameters for application as scaffolds in bone tissue regeneration. Our key result is the demonstration that coated scaffold can deliver controlled doses of strontium toward the SBF medium. That is the determinant for bone tissue regeneration, as far as strontium is known to positively act on bone remodeling.

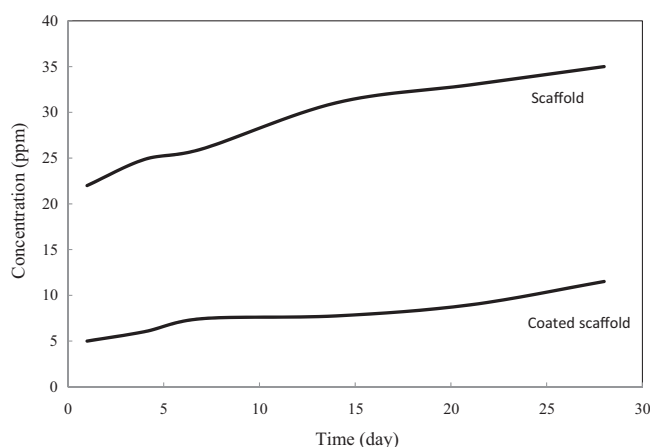


Fig. 10. Strontium ion release from coated and uncoated scaffolds as function of immersion time in SBF.

References

- Palangkaraya A, Yong J. Population ageing and its implications on aggregate health care demand: empirical evidence from 22 OECD countries. *Int J Health Care Finance Econ* 2009;**9**(4):391–402.
- Hutmacher DW. Scaffolds in tissue engineering bone and cartilage. *Biomaterials* 2000;**21**(24):2529–43.
- Moroni L, de Wijn JR, van Blitterswijk CA. Integrating novel technologies to fabricate smart scaffolds. *J Biomater Sci Polym Ed* 2008;**19**:543–72.
- Rezwani K, Chen QZ, Blaker JJ, Boccacini AR. Biodegradable and bioactive porous polymer/inorganic composite scaffolds for bone tissue engineering. *Biomaterials* 2006;**27**(18):3413–31.
- Gerhardt L-C, Boccacini AR. Bioactive glass and glass–ceramic scaffolds for bone tissue engineering. *Materials* 2010;**3**(7):3867–910.
- Hench LL. Bioceramics. *J Am Ceram Soc* 1998;**81**:1705–28.
- Hench LL. Bioceramics: from concept to clinic. *J Am Ceram Soc* 1991;**74**:1487–510.
- Yao J, Radin S, Leboy S, Ducheyne P. The effect of bioactive glass content on synthesis and bioactivity of composite poly(lactic-co-glycolic acid)/bioactive glass substrate for tissue engineering. *Biomaterials* 2005;**26**(14):1935–45.
- Hench LL, Splinter RJ, Allen WC, Greenlee TK. Bonding mechanisms at the interface of ceramic prosthetic materials. *J Biomed Mater Res* 1971;**2**:117–41.
- Chen QZ, Thompson ID, Boccacini AR. 45S5 Bioglass®-derived glass-ceramic scaffolds for bone tissue engineering. *Biomaterials* 2006;**27**:2414–25.
- Vitale-Brovarone C, Verne E, Robiglio L, Appendino P, Bassi F, Martinasso G, et al. Development of glass–ceramic scaffolds for bone tissue engineering: characterisation, proliferation of human osteoblasts and nodule formation. *Acta Biomater* 2007;**3**:199.
- Livingston T, Ducheyne P, Garino JJ. *In vivo* evaluation of a bioactive scaffold for bone tissue engineering. *Biomed Mater Res* 2002;**62**:1.
- Hench LL. Genetic design of bioactive glass. *J Eur Ceram Soc* 2009;**29**:1257–65.
- Xynos ID, Edgar AJ, Buttery LDK, Hench LL, Polak JM. Gene-expression profiling of human osteoblasts following treatment with the ionic products of Bioglass® 45S5 dissolution. *J Biomed Mater Res* 2001;**55**:151–7.
- Leach KJ, Kaigler D, Wang Z, Krebsbach PH, Mooney DJ. Coating of VEGF-releasing scaffolds with bioactive glass for angiogenesis and bone regeneration. *Biomaterials* 2006;**27**:3249–55.
- Gorustovich AA, Roether JA, Boccacini AR. Effect of bioactive glasses on angiogenesis: a review of *in vitro* and *in vivo* evidences. *Tissue Eng B* 2010;**16**:199–207.
- Chen YW, Shi GQ, Ding YL, Yu XX, Zhang XH, Zhao CS, et al. *In vitro* study on the influence of strontium-doped calcium polyphosphate on the angiogenesis-related behaviors of HUVECs. *J Mater Sci Mater Med* 2008;**19**:2655–62.
- Canalis E, Hott M, Deloffre P, Tsouderos Y, Marie PJ. The divalent strontium salt S12911 enhances bone cell replication and bone formation *in vitro*. *Bone* 1996;**18**:517–23.
- Buehler J, Chappuis P, Saffar JL, Tsouderos Y, Vignery A. Strontium ranelate inhibits bone resorption while maintaining bone formation in alveolar bone in monkeys. *Bone* 2001;**29**:176–9.
- Hott M, Deloffre P, Tsouderos Y, Marie PJ. S12911-2 reduces bone loss induced by short-term immobilization in rats. *Bone* 2003;**33**:112–23.
- Meunier PJ, Roux C, Seeman E, Ortolani S, Badurski JE, Spector TD, et al. The effects of strontium ranelate on the risk of vertebral fracture in women with postmenopausal osteoporosis. *N Engl J Med* 2004;**350**:459–568.
- Seeman E, Devogelaer JP, Lorenc R, Spector T, Brixen K, Balogh A, et al. Strontium ranelate reduces the risk of vertebral fractures in patients with osteopenia. *J Bone Miner Res* 2008;**23**:433–8.
- Gentleman E, Fredholm YC, Jell G, Lotfibakhshaiesh N, O'Donnell MD, Hill RG, et al. The effects of strontium-substituted bioactive glasses on osteoblasts and osteoclasts *in vitro*. *Biomaterials* 2010;**31**(14):3949–56.
- Gorustovich AA, Steimetz T, Cabrini RL, López JMP. Osteoconductivity of strontium-doped bioactive glass particles: a histomorphometric study in rats. *J Biomed Mater Res A* 2010;**92A**(1):232–7.
- Hesaraki S, Alizadeh M, Nazarian H, Sharifi D. Physico-chemical and *in vitro* biological evaluation of strontium/calcium silicophosphate glass. *J Mater Sci Mater Med* 2010;**21**:695–705.
- Guida A, Towler MR, Wall JG, Hill RG, Eramo S. Preliminary work on the antibacterial effect of strontium in glass ionomer cements. *J Mater Sci Lett* 2003;**22**:1401–3.
- Lao J, Jallot E, Nedelec J. Strontium-delivering glasses with enhanced bioactivity: a new biomaterial for antiosteoporotic applications. *Chem Mater* 2008;**20**:4969–73.
- Zhang M, Zhai W, Lin K, Pan H, Lu W, Chang J. Synthesis, *in vitro* hydroxyapatite forming ability, and cytocompatibility of strontium silicate powders. *J Biomed Mater Res B: Appl Biomater* 2010;**93B**:252–7.
- Wong CT, Lu WW, Chan WK, Cheung KMC, Luk KDK, Lu DS, et al. *In vivo* cancellous bone remodeling on a strontium-containing hydroxyapatite (Sr-HA) bioactive cement. *J Biomed Mater Res* 2004;**68A**:513–21.
- Li ZY, Lam WM, Yang C, Xu B, Ni GX, Abbah SA, et al. Chemical composition, crystal size and lattice structural changes after incorporation of strontium into biomimetic apatite. *Biomaterials* 2007;**28**:1452–60.
- Lakkar NJ, Abou Neel EA, Salih V, Knowles JC. Strontium oxide doped quaternary glasses: effect on structure, degradation and cytocompatibility. *J Mater Sci Mater Med* 2009;**20**:1339–46.
- Towler MR, Boyd D, Freeman C, Brook IM, Farthing P. Comparison of *in vitro* and *in vivo* bioactivity of SrO–CaO–ZnO–SiO₂ glass grafts. *J Biomater Appl* 2009;**23**:561–72.
- Cheung KMC, Lu WW, Luk KDK, Wong CT, Chan D, Shen JX, et al. Vertebroplasty by use of a strontium-containing bioactive bone cement. *Spine* 2005;**30**:84–91.
- Ni GX, Lu WW, Chiu KY, Li ZY, Fong DYT, Luk KDK. Strontium-containing hydroxyapatite (Sr-HA) bioactive cement for primary hip replacement: an *in vivo* study. *J Biomed Mater Res B* 2006;**77B**:409–15.
- Wang X, Bank RA, Tekoppele JM, Agrawal CM. The role of collagen in determining bone mechanical properties. *J Orth Res* 2001;**19**:1021.
- Yunos DM, Bretcanu O, Boccacini AR. Polymer-bioceramic composites for tissue engineering scaffolds. *J Mater Sci* 2008;**43**:4433–42.
- Peroglio M, Gremillard L, Gauthier C, Chazeau L, Verrier S, Alini M, et al. Mechanical properties and cytocompatibility of poly(ϵ -caprolactone)-infiltrated biphasic calcium phosphate scaffolds with bimodal pore distribution. *Acta Biomater* 2010;**6**:4369–79.
- Chen QZ, Efthymiou A, Salih V, Boccacini AR. Bioglass®-derived glass-ceramic scaffolds: study of cell proliferation and scaffold degradation *in vitro*. *J Biomed Mater Res A* 2008;**84**:1049–60.
- Mantsos T, Chatzistavrou X, Roether JA, Hupa L, Arstila H, Boccacini AR. Non-crystalline composite tissue engineering scaffolds using boron-containing bioactive glass and poly(D,L-lactic acid) coatings. *Biomed Mater* 2009;**4**:055002–14.
- Nalla RK, Kinney JH, Ritchie RO. Mechanistic fracture criteria for the failure of human cortical bone. *Nat Mater* 2003;**2**:164.
- Nalla RK, Kinney JH, Ritchie RO. Mechanistic aspects of fracture and R-curve behavior in human cortical bone. *Biomaterials* 2003;**24**:3955.
- Gorgieva S, Kokol V. Biomaterials applications for nanomedicine (Chapter 2). In: Pignatello R, editor. *Collagen- vs. gelatin-based biomaterials and their biocompatibility: review and perspectives*. 2011. p. 17–52.
- Erol M, Özyüğüran A, Özarpaz Ö, Küçükbayrak S. Investigation of strontium effect on the bioactive behavior of glasses in the system SiO₂–CaO–P₂O₅–Na₂O–SrO. *Key Eng Mater* 2012;**493–494**:68–73.
- Kokubo T, Huang ZT, Hayashi T, Sakka S, Kitsugi T, Yamamuro T. Ca, P-rich layer formed on high-strength bioactive glass–ceramic A-W. *J Biomed Mater Res* 1990;**24**:331–43.
- Hollister S. Porous scaffold design for tissue engineering. *Nat Mater* 2005;**4**:518–24.
- Agrawal CM, Ray RB. Biodegradable polymeric scaffolds for musculoskeletal tissue engineering. *J Biomed Mater Res* 2001;**55**:141–50.
- Hollinger JO, Brekke J, Gruskin E, Lee D. Role of bone substitutes. *Clin Orthop Relat Res* 1996;**324**:55–65.

48. Mansur HS, Costa HS. Nanostructured poly(vinyl alcohol)/bioactive glass and poly(vinyl alcohol)/chitosan/bioactive glass hybrid scaffolds for biomedical applications. *Chem Eng J* 2008;**137**:72–83.
49. Zhang W, Shen Y, Pan H, Lin K, Liu X, Darvell BW, et al. Effects of strontium in modified biomaterials. *Acta Biomater* 2011;**7**:800–8.
50. Cabrera WE, Schrooten I, De Broe ME, D'Haese PC. Strontium and bone. *J Bone Min Res* 1999;**14**:661–8.
51. Bretcanu O, Chatzistavrou X, Paraskevopoulos K, Conradt R, Thompson I, Boccaccini AR. Sintering and crystallisation of 45S5 Bioglass® powder. *J Euro Ceram Soc* 2009;**29**:3299–306.
52. Lefebvre L, Gremillard L, Chevalier J, Zenati R, Bernache-Assollant D. Sintering behaviour of 45S5 Bioactive glass. *Acta Biomater* 2008;**4**:1894–903.
53. Lefebvre L, Chevalier J, Gremillard L, Zenati R, Thollet G, Bernache-Assollant D, et al. Structural transformations of bioactive glass 45S5 with thermal treatments. *Acta Mater* 2007;**55**:3305–13.
54. Wu C, Ramaswamy Y, Boughton P, Zreiqat H. Improvement of mechanical and biological properties of porous CaSiO₃ scaffolds by poly(D,L-lactic acid) modification. *Acta Biomater* 2008;**4**:343–53.
55. Mouriño V, Newby P, Boccaccini AR. Preparation and characterization of gallium releasing 3-D alginate coated 45S5 Bioglass® based scaffolds for bone tissue engineering. *Adv Eng Mater* 2010;**12**:B283–91.
56. Peroglio M, Gremillard L, Chevalier J, Chazeau L, Gauthier C, Hamaide T. Toughening of bio-ceramics scaffolds by polymer coating. *J Euro Ceram Soc* 2007;**27**:2679–85.
57. Bonnelye E, Chabadel A, Saltel F, Jurdic P. Dual effect of strontium ranelate: stimulation of osteoblast differentiation and inhibition of osteoclast formation and resorption *in vitro*. *Bone* 2008;**42**:129–38.
58. Reginster JY, Meunier PJ. Strontium ranelate phase 2 doseranging studies: PREVOS and STRATOS studies. *Osteoporos Int* 2003;**14**:56–65.
59. Schrooten I, et al. Dose-dependent effects of strontium on bone of chronic renal failure rats. *Kidney Int* 2003;**63**:927–35.
60. Murphy S, Boyd D, Moane S, Bennett M. The effect of composition on ion release from Ca–Sr–Na–Zn–Si glass bone grafts. *J Mater Sci: Mater Med* 2009;**20**:2207–14.